PHYSICS WITH η MESONS

V.S.Bekrenev, S.P.Kruglov, I.V.Lopatin

Introduction

The program "Physics with η mesons" is a logical continuation of a series of experiments on studying pion-nucleon interaction, which were under way at PNPI starting from 1970.

The η meson differs essentially by its properties from the π meson. The major difference is in the isospin ($I = 0$ for the η meson and $I = 1$ for the π meson). As a consequence, the ηN system couples only to the N^* resonances – in contrast with the πN system which couples to both the N^* and Δ resonances. The π meson being consisted of only the u and q quarks, the η meson contains additionally the s quark; it explains why the η meson is four times heavier than the π meson.

Because of the short lifetime of the η meson (6×10^{-19} s) it is impossible to get beams of these particles, and the only way to obtain an experimental information about the character of the interaction of η mesons with nucleons and nuclei is to study processes of η production caused by different projectiles. Up to now such information is absent practically.

PNPI has good opportunities for studying pion-induced processes of η production. As to the elementary process $\pi^- p \to \eta n$, the threshold of this reaction is 685 MeV/c; the total cross section rises sharply from the threshold reaching the maximum value $\sigma_{tot} \simeq 2.5$ mb at $p = 760$ MeV/c. For (π, η) reactions on nuclei the threshold is essentially lower. A pion channel of the PNPI synchrocyclotron allows to get intense pion beams just in the momentum region from the threshold up to the maximum of the cross section.

Study of η production on nucleons

The first stage of the program is studying the process $\pi^- p \to \eta n$ in the near-threshold region. A detailed investigation of the cross section of this process *vs* momentum of incident pions will allow to obtain information about such fundamental constant of the ηN interaction as the ηN scattering length. In contrast with the πN system, the ηN scattering length is positive, that is the ηN interaction has the attractive character. This feature allows to hope that ηN bound states (η-mesic nuclei) exist – if the scattering length is big enough. At present, different analyses using experimental data on the pion-induced and gamma-induced η production result in real parts of the scattering length lying in the range from 0.3 to 0.9 fm. More accurate determination of this value will have decisive importance for estimating a possibility of the existence of the η-mesic nuclei.

Data obtained as a result of these experiments will be used also for testing the theoretical model of coupled channels $\pi N \to \pi N$, $\pi N \to \pi\pi N$ and $\pi N \to \eta N$, which was proposed by L.C.Liu et al. (1988) for the combined description of processes of πN interaction and η production.

Experiments on measuring yields of the process $\pi^- p \to \eta n$ were carried out in the pion channel of the PNPI synchrocyclotron by detecting emitted recoil neutrons and determining their energies by means of time-of-flight technique.

The kinematics of the process $\pi^- p \to \eta n$ in the near-threshold region is such that all the neutrons are emitted in the laboratory system in the forward direction, in a relatively small

cone. The maximum angle of their emission increases with the momentum of the incident pions, the most of neutrons being emitted at angles close to the maximum one. Another feature of this process is that for a given angle in the laboratory system θ_n^{lab} two groups of neutrons with different energies (corresponding to the neutron emission to the forward and to the backward hemispheres in the centre-of-mass system) are detected.

In the near-threshold region the η production occurs only in the S-state. Under this supposition, number of detected neutrons is defined by the equation:

$$N = N_\pi N_p \varepsilon_n \sigma_{tot} A_n \quad , \tag{1}$$

where N_π – the number of the incident pions; N_p – the number of protons in a target ($1/\mathrm{cm}^2$); ε_n – the efficiency of neutron detectors; σ_{tot} – the total cross section of the investigated process; A_n – the angular acceptance (that is the fraction of the total solid angle in the c.m.s. subtended by the neutron detector). Evidently, the product of the two functions, one of which, σ_{tot}, steeply rises and the other, A_n, falls with momentum of the incident pions, gives a dependence characterized by a peak. For real experimental conditions this dependence is to be averaged over a momentum spread of the beam.

The experiment on measuring yields of the reaction $\pi^- p \to \eta n$ [1] has been carried out in the pion channel of the PNPI synchrocyclotron by the Russian-American collaboration which included, besides PNPI physicists, scientists of the University of California at Los Angeles and Abilene Christian University (USA). The experimental layout is presented in Fig. 1. A liquid hydrogen target of vacuum type was used in the experiment. A hydrogen flask is a vertical cylinder 10 cm in diameter and 12 cm high, its walls are made of aluminum 0.1 mm thick. The liquefaction of hydrogen in the flask was performed by its cooling with liquid helium.

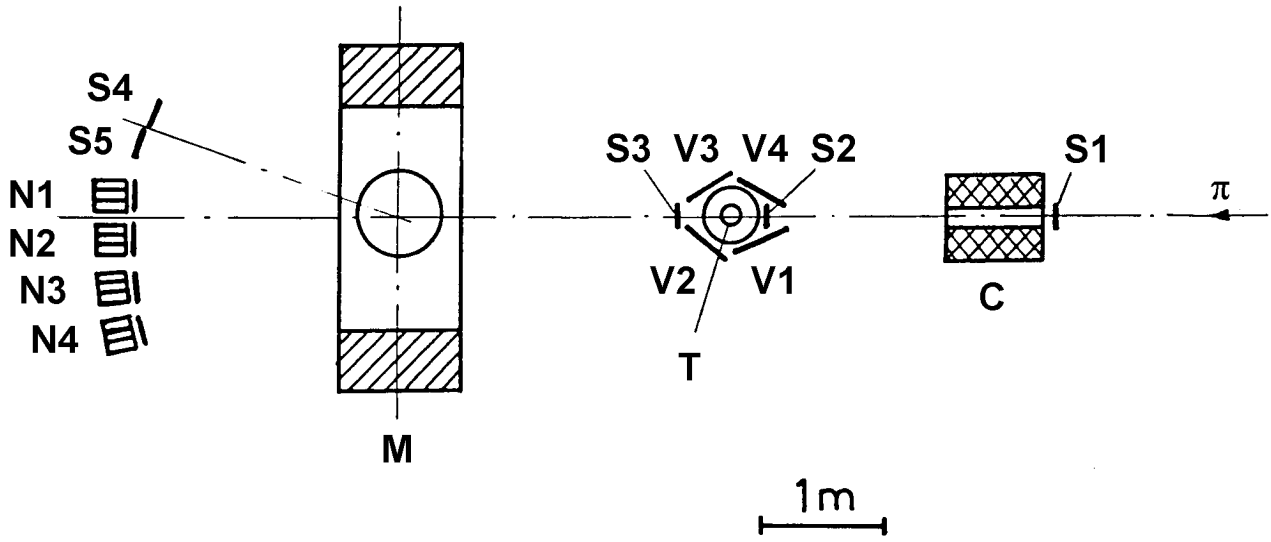

Fig. 1. Experimental layout. T – liquid hydrogen target; N1–N4 – neutron detectors; S1, S2 – monitor counters; S3, S4, S5 – veto counters placed on the incident beam axis; V1–V4 – veto counters around the target; M – deflecting magnet.

Neutron detectors were designed and manufactured at the University of California at Los Angeles. The detector consists of three contiguous scintillator blocks having each size

$25.4 \times 25.4 \times 8.9$ cm ^{3} (the last figure – width). Each block is viewed by two photomultiplier tubes connected in coincidence. The length of the scintillator is sufficient to provide a detection efficiency for single neutrons of more than 0.2. The neutron detectors were previously calibrated with tagged neutrons from the reaction $\pi^- d \to nn$ with the energy from 83 to 290 MeV; an accuracy of this calibration is $\pm 3.5\%$.

To lower the level of the background due to neutrons from reactions with more than two particles in the final state (such as $\pi^- p \to \pi^+ \pi^- n$ or $\pi^- p \to \pi^+ \pi^- \pi^0 n$), the target was surrounded with scintillation veto counters covering solid angle approximately 1.5 sr. Firing of any veto counter caused by crossing the scintillator by a charge particle produced a veto-signal and prevented triggering.

The total momentum acceptance of the PNPI pion channel is $\Delta p/p = 6\%$ (FWHM). Since near the threshold the total cross section of the investigated process rises sharply with the momentum of the incident pions, it is desirable to divide the total accepted momentum range into several more narrow bins while performing measurements. To do this, a hodoscope of eight narrow vertical scintillation counters (not shown in Fig. 1) was located in the place where the pion beam had the biggest momentum dispersion. Each counter of the hodoscope covers momentum bin $\Delta p/p = 1.5\%$.

When carrying out this experiment, the momentum acceptance of the pion channel was reduced by placing 4-cm momentum slit just upstream of the hodoscope of beam counters. In another words, only two central (nearest to the beam axis) counters H4 and H5 were in action.

Measurements were made at central momenta of the pion beam 670, 680, 690, 695, 700, and 710 MeV/c. At each central momentum data taking was performed simultaneously for the two momentum bins corresponding to the beam counters H4 and H5.

Yields of the η production process were determined by detecting the recoil neutrons. Selection of neutrons produced just in the reaction $\pi^- p \to \eta n$ was made by measuring their time of flight on the base between the monitor counter (located just upstream of the hydrogen target) and the corresponding neutron detector. An example of a time-of-flight spectrum is shown in Fig. 2; the number of neutrons is normalized to one incident pion. One can see the strong

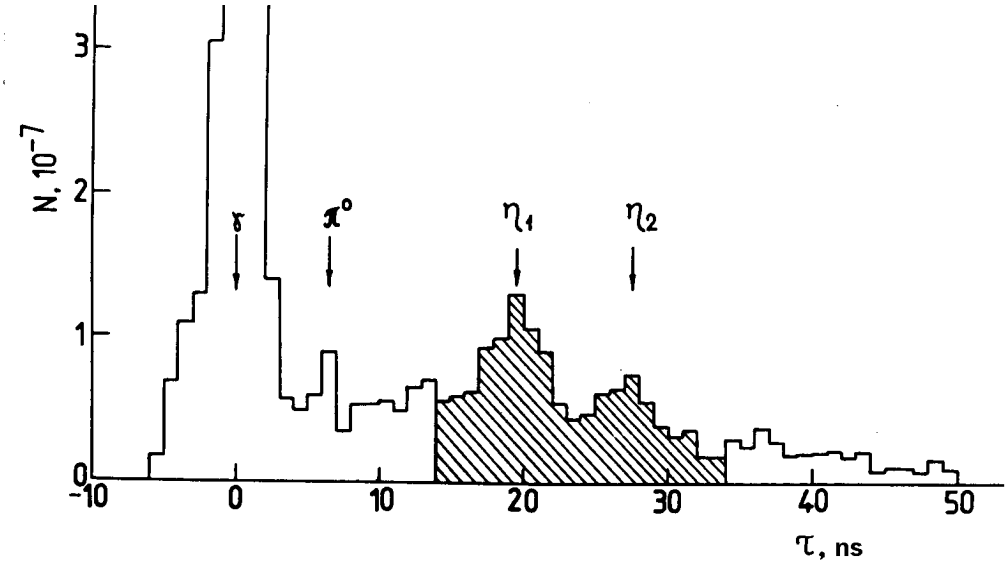

Fig. 2. Time-of-flight spectrum registered by one of neutron counters.

first peak caused by gammas from the π^0- and η-decay entering the detector; for convenience of further processing the abscissa scale is shifted in such a manner that TOF = 0 coincides with the first peak. The second peak is produced by neutrons from the reaction $\pi^- p \to \pi^0 n$, the third and fourth peaks (η_1 and η_2) are due to neutrons emitted is the reaction $\pi^- p \to \eta n$ to the forward and to the backward hemispheres in the c.m.s. A rather big continuous background ("pedestal") under these peaks is formed by neutrons produced in such reactions as $\pi^- p \to \pi^0 \pi^0 n$, $\pi^- p \to \pi^+ \pi^- n$ and so on. To extract the number of "good" events attributed to the process under study, it is necessary to subtract this background.

We used a simplified algorithm of processing, namely: instead of determining the number of "good" events (area under η peaks in Fig. 2) we counted the total number of events N_w in the TOF-"window" of 14 to 34 ns (shaded area in Fig. 2) covering both η peaks and then plotted the value N_w against the momentum of the incident pions. The obtained dependence is a superposition of the curve of the η yield and the pedestal due to reactions of pion production such as $\pi^- p \to \pi^0 \pi^0 n$. The shape of this pedestal in the rather small investigated momentum range can be approximated by a straight line the slope of which was determined from the analysis of TOF-"tails" being far from the η peaks. After subtracting the pedestal we have obtained momentum dependences of the η yield presented in Fig. 3. Error bars are the quadrature sums of statistical uncertainties and systematic ones due to the procedure of the pedestal subtraction. Maxima of the measured dependences shift to higher momentum when the angle of the neutron emission increases – this maximum is located at $p \simeq 690$ MeV/c for $\theta_n^{lab} = 0.9°$ and at $p \simeq 710$ MeV/c for $\theta_n^{lab} = 10.5°$.

Shown by curves in Fig. 3 are results of calculations performed using expression (1). The value of the angular acceptance A_n was obtained by a Monte Carlo simulation taking into account a real geometry of the experiment and measured spatial characteristics of the pion beam; the value of the η mass $M_\eta = 547.45$ MeV/c^2 was taken from the last Tables of the Particle Data Group. While calculating we used – as a first approximation – the momentum dependence of the total cross section $\sigma_{tot}(p)$ obtained by fitting published experimental data in an assumption that the process $\pi^- p \to \eta n$ occurs through an excitation of the $S_{11}(1535)$ resonance. Calculated dependences are normalized in maxima to measured ones. It can be seen that the calculations reproduce the shape of the momentum dependences rather well. It may be considered as an indication that the PNPI experimental data agree with the above mentioned value of the η mass and that the used fitting $\sigma_{tot}(p)$ reflects adequately the real momentum dependence of the cross section. On the other hand, the good agreement between the calculation and the experiment confirms [2] the correctness of the absolute momentum scale calibration of the PNPI pion channel – the shifts of the calculated curves relatively to the measured dependences do not exceed 0.5% (3.5 MeV/c) that is within the accuracy of the momentum scale calibration performed earlier [3].

It can be shown that the value of difference $\Delta\tau$ between positions of the two peaks η_1 and η_2 in the TOF spectra is very sensitive to the incident pion momentum in the near-threshold region. For example, for $\theta_n^{lab} = 0.93°$ this value varies from 7.4 ns to 16.6 ns when the incident momentum changes from 690 MeV/c to 710 MeV/c. It means that precise measurements of $\Delta\tau$ may be used for determining the pion beam momentum. In particular, this method was applied at PNPI [4] in order to determine values of the incident momentum p_i which correspond to pions crossing the ith counter of the beam hodoscope. The resulted values of p_i agree with ones obtained using the special Monte Carlo program "MESON" developed at PNPI for the calculation of characteristics of meson beams.

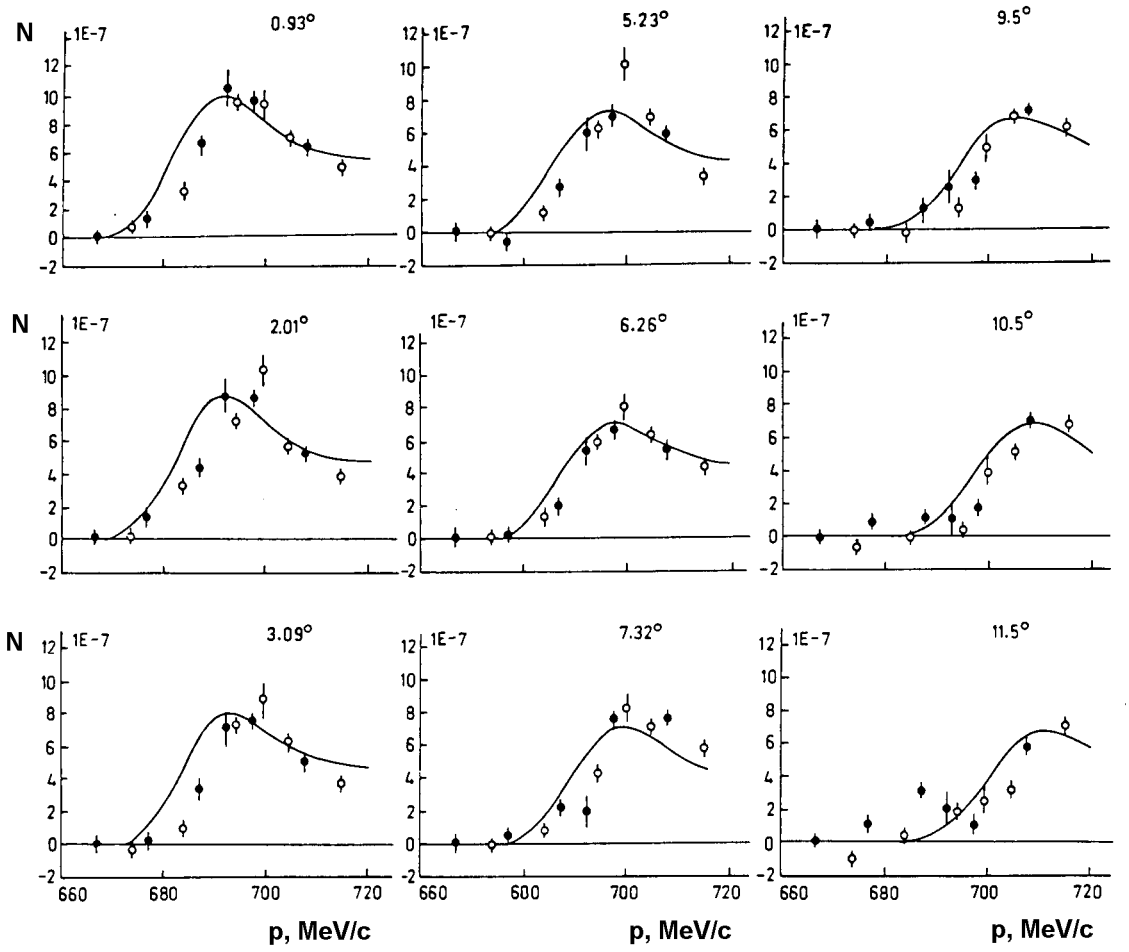

Fig. 3. Yields of the reaction $\pi^- p \to \eta n$ for different angles of neutron emission. Experimental points shown by open and solid circles correspond to the beam counters H4 and H5, respectively.

Measurement of cross sections of $\pi^- p$ charge exchange scattering in the region of η production threshold

The next stage of the program – measurement of the differential cross sections of $\pi^- p$ charge exchange scattering in the momentum range from 415 to 725 MeV/c [5]. One of main goals of this series of experiments is to study cusp effects in the reaction $\pi^- p \to \pi^0 n$ in the region of the η production threshold. The opening of the new inelastic channel $\pi^- p \to \eta n$ should result in appearing cusps in the momentum dependence of the differential cross sections of the reaction $\pi^- p \to \pi^0 n$. A detailed measurement of this dependence in the vicinity of the η production threshold will allow to reconstruct the amplitude of $\pi^- p$ charge exchange scattering at the momentum corresponding to the η threshold ($p = 685$ MeV/c). Comparison of this amplitude with that extracted from experimental data by means of a phase shift analysis will be a good test of both the correctness of the analysis procedure and validity of suppositions and approximations used while performing this analysis.

The analysis of time-of-flight spectra (Fig. 2) shows that the neutrons from the reaction $\pi^- p \to \pi^0 n$ manifest themselves as a peak seen over a rather big background, and the subtraction of this background leads to a large systematic error when determining the number of neutrons produced in this reaction. To lower this error, we decided to detect the neutron in coincidence with one of gammas from the decay $\pi^0 \to 2\gamma$. A dramatic effect of $n\gamma$-coincidences is illustrated by Fig. 4 demonstrating how the initial time-of-flight spectrum is modified when these coincidences are used. It is seen that the first strong peak and the background are suppressed essentially and the neutrons from the $\pi^- p$ charge exchange reaction are selected very clearly. [1]

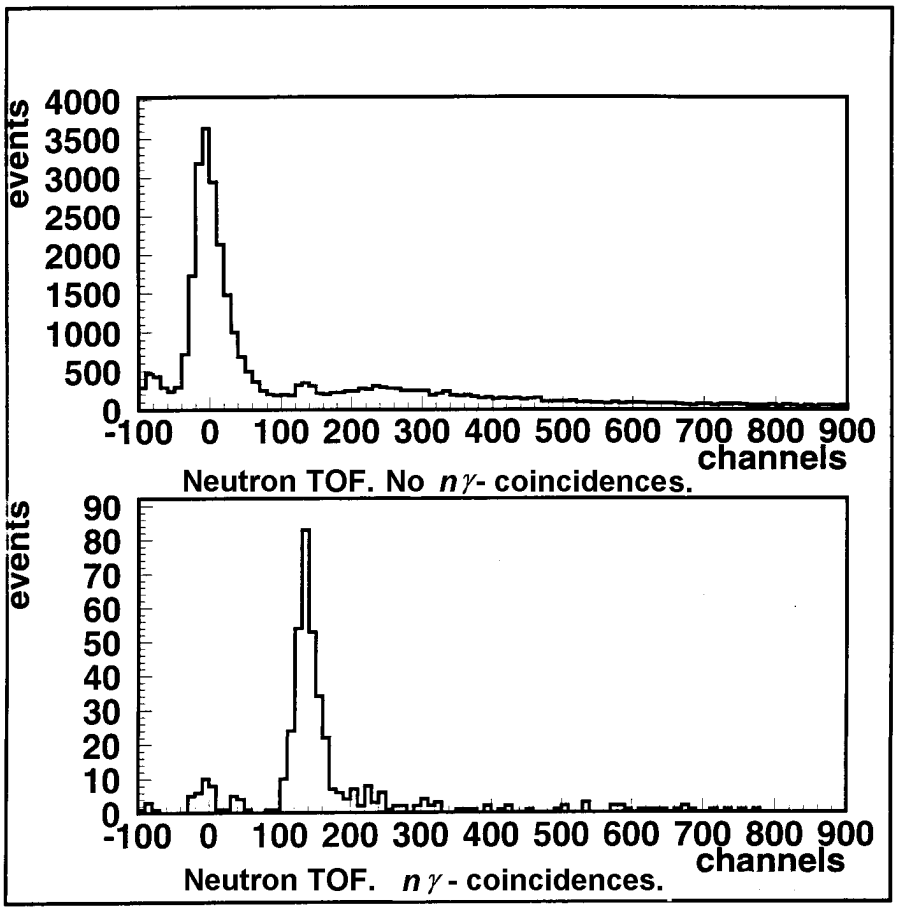

Fig. 4. Time-of-flight neutron spectra before (top) and after (bottom) using $n\gamma$-coincidences.

A schematic view of the experimental setup is shown in Fig. 5. The disposition of neutron detectors in the first series of measurements is the same as in the previous experiment, thus the cross sections of $\pi^- p$ charge exchange scattering to the backward hemisphere (for angles 150° to 180° in the c.m.s.) are measured. Gamma detectors are placed at angles kinematically conjugated with the neutron detectors. Two different types of total absorption electromagnetic calorimeters were used as gamma detectors. The first detector is the Čerenkov spectrometer

[1] It should be emphasized that different ordinate scales are used in top and bottom graphs.

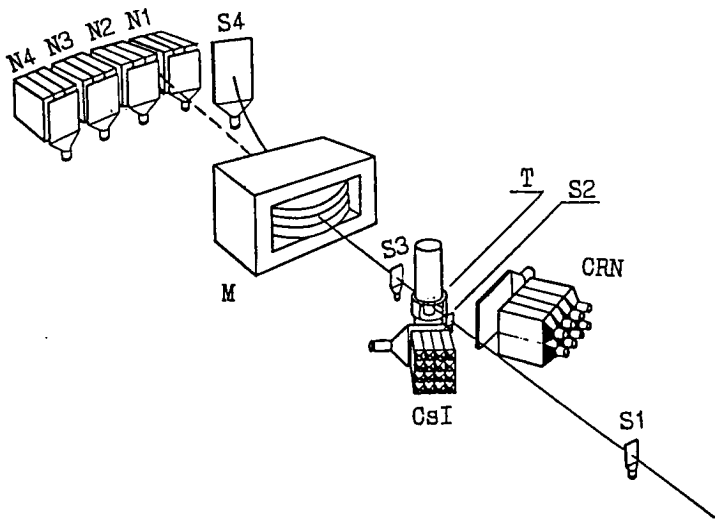

Fig. 5. Schematic drawing of the setup for measuring cross sections of $\pi^- p$ charge exchange scattering. S1, S2 – monitor counters; S3, S4 – beam veto counters; N1–N4 – neutron detectors; M – magnet deflecting incident pion beam; T – liquid hydrogen target; CsI – gamma-detector consisting of 16 crystals CsI(Na); CRN – gamma-detector consisting of 8 Čerenkov lead glass blocks.

made of eight lead glass SF-5 blocks (with individual size $15 \times 15 \times 35$ cm^3) arranged in a 4×2 array and the second one consists of sixteen (4×4) crystals CsI(Na) each having size $6 \times 6 \times 30$ cm^3. The thickness of the calorimeters corresponds to 14 r.l. and 16 r.l., respectively. Upstream of the gamma detectors veto counters rejected charged particles were placed.

After the number of $n\gamma$-coincidences $N_{n\gamma}$ is measured in an experiment, the differential cross section of the reaction $\pi^- p \to \pi^0 n$ in the centre-of-mass system may be determined using the expression:

$$\frac{d\sigma}{d\Omega} = \frac{N_{n\gamma}}{N_\pi N_p \Delta\Omega_n^{lab} J_n \varepsilon_n F_\gamma}, \tag{2}$$

where N_π is the number of pions passing through the liquid hydrogen target during the beam run; N_p is the number of protons in the target (1/cm^2); $\Delta\Omega_n^{lab}$ is the lab. solid angle subtended by the neutron detector; J_n is the neutron Jacobian; ε_n is the efficiency of the neutron detector. The coefficient F_γ means what fraction of all gammas from the decay of π^0 mesons kinematically conjugated with neutrons in the solid angle $\Delta\Omega_n^{lab}$ are detected by the gamma detectors; this coefficient was determined by a Monte Carlo simulation taking into account a real geometry of the experiment, spatial characteristics of the incident pion beam, an energy resolution and a registration threshold of the gamma-detectors.

To eliminate the contribution due to charge exchange scattering of the incident pions on the scintillator of the monitor counter and elements of the target construction, for every central momentum measurements were made for both the hydrogen-filled and empty target; then channel-by-channel subtraction of corresponding TOF-spectra was performed – after normalization to one incident pion.

Preliminary results of processing of data obtained in the first beam run are presented in Fig. 6; only statistical errors are shown. Some irregularities in the momentum dependence of $d\sigma/d\Omega$ seen in the region of the η-production threshold (p = 685 MeV/c) reflect cusp effects mentioned in the beginning of this section. For more detailed investigation of these effects measurements with the better momentum resolution are needed.

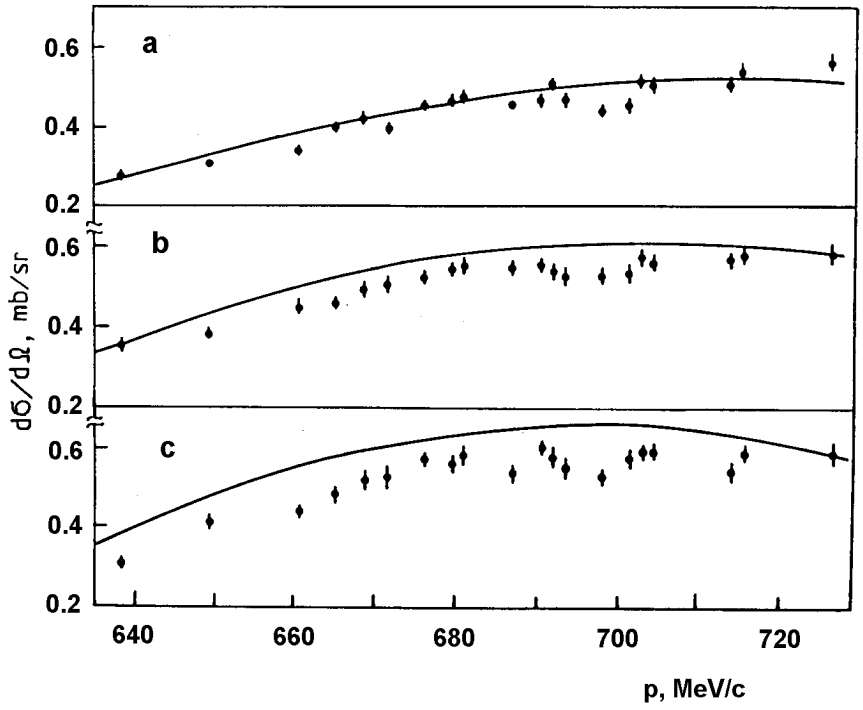

Fig. 6. Preliminary results of measuring the differential cross sections of $\pi^- p$ charge exchange scattering for three angles in the c.m.s.: a) 157°; b) 166°; c) 175.5°. Shown by curves are the predictions of the phase shift analysis PNPI–94.

Obtained precise values of the differential cross sections of $\pi^- p$ charge exchange scattering will allow to estimate quantitatively the charge splitting effect in the P_{33} phase shifts. Such splitting was discovered for the first time at PNPI as a result of the phase shift analysis PNPI–94, however its detailed investigation is prevented by an insufficient accuracy of determining the P_{33} phase shifts for $\pi^- p$ scattering that, in turn, is due mainly to a lack of precise experimental data on the differential cross sections of $\pi^- p$ charge exchange scattering. Besides, the measured momentum dependences of these cross sections will be used for extracting information about the cusp effects in $\pi^- p$ charge exchange scattering and about the amplitude of this reaction at the momentum of the incident pions corresponding to the η production threshold.

Development of the η-meson spectrometer

Investigation of processes of η production on nucleons and nuclei requires development of a novel detector – called usually η spectrometer – allowing not only to detect the η meson but also to determine its energy with a high precision. A prototype of the η spectrometer consisting of two calorimeters with sixteen crystals CsI(Na) in each one (in configuration 4×4) was designed and created recently at PNPI. The size of the individual crystal is $6 \times 6 \times 30$ cm^3.

The energy calibration of the calorimeters was made using electrons of different energies, which were produced in the pion channel of the PNPI synchrocyclotron. Obtained results [7] are shown in Fig. 7. One can see that the energy resolution $\Delta E/E$ (FWHM) for a single crystal varies from 18% to 16% when the energy of electrons rises from 100 to 250 MeV; for a cluster of 9 crystals the value $\Delta E/E$ is equal 13% and 10%, respectively.

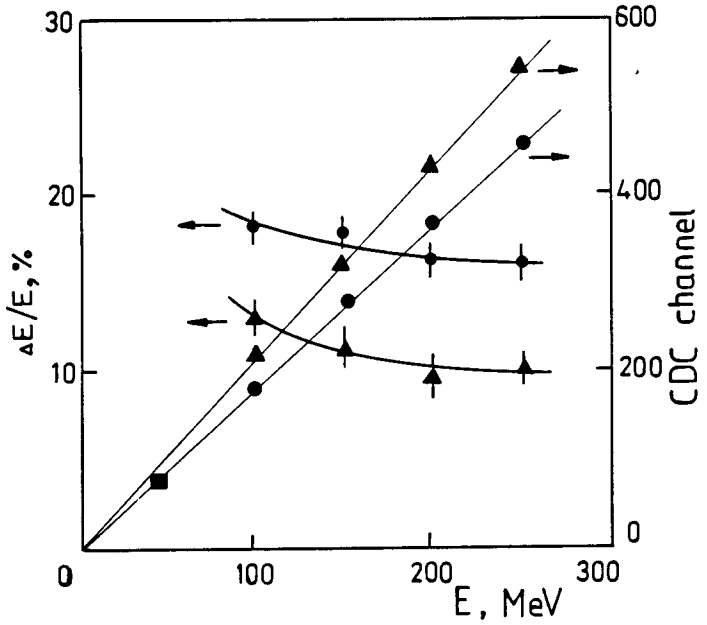

Fig. 7. The position of the peak in the pulse height spectrum (straight lines) and the energy resolution (curves) *vs* the energy of electrons incident on the calorimeter. Data for a central crystal are shown by circles, results obtained by summing signals from nine crystals (including central one) – by triangles. Shown also (by square) is the position of the peak caused by the cosmic muons.

The method of the gain equalization of different CsI(Na) modules was developed on the basis of cosmic ray spectra. While passing through a crystal, cosmic muons deposit the energy approximately 40 MeV producing a clear peak in the pulse height spectrum. The applied voltages for all PMTs are adjusted in such a manner that for all the crystals this peak would be at one and the same channel of a charge-to-digital convertor (CDC). In further, this peak caused by the cosmic muons was used for monitoring the long-term stability of the individual CsI(Na) counters in the course of experiments.

The main principle of the η spectrometer is to measure energies E_1 and E_2 of two gammas from the decay of η meson and their opening angle ψ. After these values are known, the kinetic

energy of η meson can be obtained using the equation

$$E_\eta = \left[\frac{2M_\eta^2}{(1-\cos\psi)(1-X^2)}\right]^{1/2} - M_\eta\,, \qquad (3)$$

where M_η is the η mass and $X = (E_1 - E_2)/(E_1 + E_2)$ characterizes the sharing of energy between the two gammas. It may be shown that in the case of the symmetric gamma emission ($X \leq 0.1$) and for the energy resolution for the gammas $\Delta E/E \simeq 10\%$ and the angular accuracy $\Delta\psi \simeq 50$ mrad we can determine the energy of the η meson with an uncertainty of 2.5 MeV for $E_\eta = 100$ MeV. This uncertainty can be essentially lowered if the accuracy $\Delta\psi$ is improved.

The above described η spectrometer is aimed to detect π^0 and η mesons *via* their decay into two gammas. For measuring processes $\pi^- p \to \pi^0\pi^0 n$, $\pi^- p \to \pi^0\eta n$ and others in which three, four and more gammas are produced a detector with an angular acceptance close to 4π is needed. These reactions will be studied in joint experiments E913/E914 at the Brookhaven National Laboratory (USA) using the Crystal Ball; these experiments have started already in April 1997.

References

[1] *I.V.Lopatin, V.V.Abaev, V.S.Bekrenev, E.A.Filimonov, A.B.Gridnev, M.R.Kan, N.G.Kozlenko, S.P.Kruglov, L.V.Lapochkina, A.Yu.Majorov, A.B.Starostin, V.V.Sumachev, B.M.K.Nefkens, J.W.Price, D.B.White, R.M.Clajus, M.E.Sadler, L.D.Isenhower, S.E.Garner, J.R.Phillips, J.A.Redmon.* // Proc. Int. Conf. on Physics with GeV-Particle Beams, 22 – 25 August 1994, Jülich, Germany, P.120.

[2] *I.V.Lopatin, V.V.Abaev, V.S.Bekrenev, A.B.Gridnev, M.R.Kan, N.G.Kozlenko, S.P.Kruglov, L.V.Lapochkina, A.Yu.Majorov, A.B.Starostin, V.V.Sumachev, E.A.Filimonov, B.M.K.Nefkens, J.W.Price, D.B.White, R.M.Clajus, M.E.Sadler, L.D.Isenhower, S.E.Garner, J.R.Phillips, J.A.Redmon.* // Prib. Tekh. Eksp., 1995. No 1. P.15.

[3] *V.A.Gordeev, A.B.Gridnev, V.P.Koptev, S.P.Kruglov, L.A.Kuz'min, I.V.Lopatin.* // Prib. Tekh. Eksp., 1976. No 2. P.25.

[4] *N.G.Kozlenko, V.V.Abaev, V.S.Bekrenev, S.P.Kruglov, I.V.Lopatin, A.B.Starostin, D.Isenhower, M.Sadler, R.Chrien, R.Sawafta, R.Sutter, M.Clajus, A.Marisic, S.McDonald, B.Nefkens, B.Tippens, D.White, W.Briscoe, T.Morrison, Z.Papandreou, A.Effendiev.* // Bull. Amer. Phys. Soc., 1996. V.41. P.1270.

[5] *I.V.Lopatin, V.V.Abaev, V.S.Bekrenev, E.A.Filimonov, A.B.Gridnev, M.R.Kan, N.G.Kozlenko, S.P.Kruglov, L.V.Lapochkina, A.Yu.Majorov, D.V.Novinsky, A.B.Starostin, V.V.Sumachev, B.M.K.Nefkens, J.W.Price, D.B.White, R.M.Clajus, M.E.Sadler, L.D.Isenhower, S.E.Garner, J.R.Phillips, J.A.Redmon.* // Few Body Systems Suppl., 1995. V.9. P.241.

[6] *V.V.Abaev and S.P.Kruglov.* // Z. Phys., 1995. V.A352. P.85.

[7] *V.S.Bekrenev, S.P.Kruglov, I.V.Lopatin, A.B.Starostin, E.A.Filimonov.* Preprint PNPI–1982, Gatchina, 1994. 28 p.